

Properties of Broad and Narrow Line Seyfert galaxies selected from SDSS

Vivek Kumar Jha^{*1}, Hum Chand², and Vineet Ojha¹

¹Aryabhata research institute of observational sciences (ARIES), Nainital, Uttarakhand, India

²Central University of Himachal Pradesh (CUHP), Dharamshala, Himachal Pradesh, India

Abstract

A comparative study of a representative sample of Broad and Narrow line Seyfert galaxies is presented. These galaxies have been selected from the 16th data release of the Sloan Digital Sky Survey (SDSS-DR16). Some of the properties derived from single epoch spectrum vary significantly between the two populations. We find that the emission regions of Narrow line Seyfert galaxies are rich in iron content and the accretion rate is higher compared to the Broad line Seyfert galaxies. In our analysis, the $H\beta$ emission line is found to be asymmetric in few of the galaxies with more number of Narrow-line Seyfert 1 (NLSy1) galaxies showing blue asymmetries i.e. traces of outflowing gas as compared to the Broad-line Seyfert 1 (BLSy1) galaxies. This behaviour may be explained by the higher iron content present in the emission line regions of NLSy1 galaxies.

Keywords: *galaxies: active – galaxies: nuclei – galaxies: Seyfert*

1. Introduction

Seyfert galaxies are characterized by a lower luminous active nucleus as compared to the general quasar population. Among the Seyfert galaxies, Type-1 galaxies show both narrow and broad emission lines (see [Netzer, 2015](#), for a review). These lower luminous Type-1 galaxies are subdivided into narrow and broad line Seyfert classes based on the Full Width at Half Maximum (FWHM) of the $H\beta$ emission line. NLSy1 galaxies are understood to be a subclass of active galactic nuclei (AGN) which have narrower broad Balmer line widths with FWHM of broad $H\beta$ emission line ≤ 2000 km/sec⁻¹, a small intensity ratio of the [O III] $\lambda 5007$ to $H\beta$ line ($[OIII]/H\beta \leq 3$), stronger optical Fe II emissions (see [Rakshit et al., 2017](#), and references therein), and usually steeper soft X-ray spectra and more rapid X-ray and sometimes optical flux variability (see [Ojha et al., 2020a](#)). It is assumed that these properties are due to the central black hole being less massive, but accreting at a very high rate. Low optical variability has also been reported in NLSy1 galaxies by [Rakshit & Stalin \(2017\)](#). It has been proposed by [Mathur \(2000\)](#) that the NLSy1 galaxies are a subcategory of BLSy1 galaxies only and can be assumed to be in evolutionary stages, while in [Gaskell \(2000\)](#) unusually high Fe-II strength, R_{fe} in NLSy1 galaxies is attributed to weak Balmer lines originating from a dense environment. The NLSy1 galaxies have been proposed as younger versions of the general broad line active galaxies.

The region responsible for the generation of broad emission lines is known as the Broad line Region (BLR). About 120 AGN been studied using the reverberation mapping technique (see [Bahcall et al., 1972](#), [Blandford & McKee, 1982](#)), which is a powerful time domain method to probe the inner regions of type 1 galaxies. However, with the known number of AGN extending into hundreds of thousands, thanks to the all sky surveys such as the Sloan Digital Sky Survey (SDSS) ([York et al., 2000](#)) but precise knowledge of the structure and kinematics of BLR through reverberation mapping available for only a handful of AGN (see [Bentz & Katz, 2015](#), for a comprehensive database of reverberation mapped AGN), studies have relied on statistical analysis on a selected sample of AGN constrained by

*vivek@aries.res.in, Corresponding author

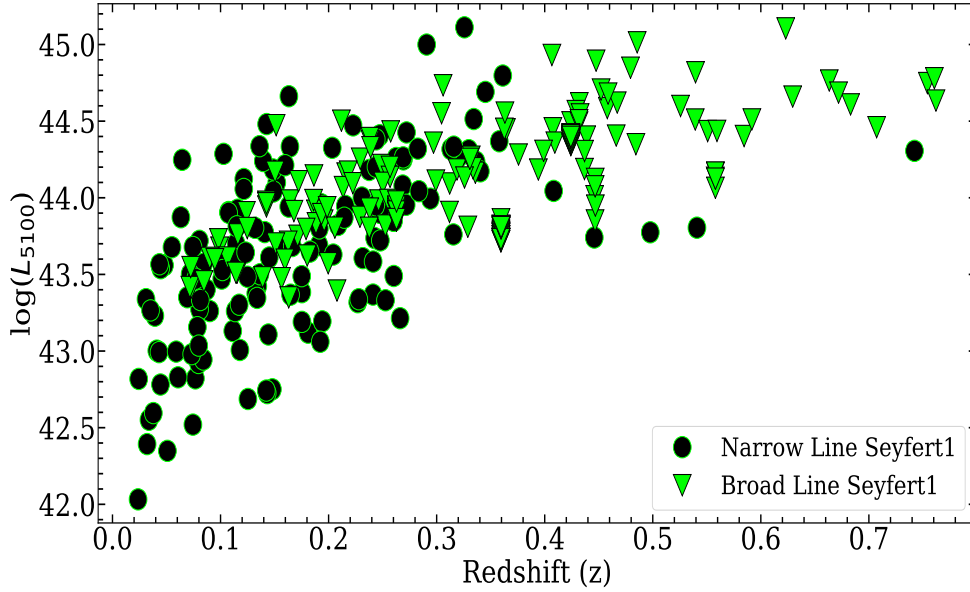


Figure 1. A representative sample of BLSy1 (green triangle) and the NLSy1 galaxies (black circle) galaxies matching in luminosity and redshift (L - z) plane being used for this work. The limit of redshift is put at 0.8 for clear $H\beta$ emission line detection in SDSS.

various limits, to infer the physical properties. A remarkable work was done by by [Boroson & Green \(1992\)](#), where they performed a Principal Component Analysis (PCA) on properties derived from X-ray, optical and radio wavelength data for a set of 87 quasars. They derived that the Eigenvector1 (E1), driven by the anti correlation of the ratio R_{Fe} of equivalent width (EW) of FeII emission lines in the optical band and the FWHM of $H\beta$ emission line is the primary cause of variability in the parameters. Since then, various aspects of E1 involving a variety of data sets as well multi-frequency parameters have been discussed in multiple works (see [Marziani et al., 2018](#), and references therein). [Sulentic et al. \(2000\)](#) and later [Zamfir et al. \(2010\)](#) established the foundations of the four-dimensional EV1 (4DE1) formalism, including the (FWHM) of $H\beta$ and R_{fe} as two of the main components. These two quantities are respectively related to the black hole mass and the Eddington ratio and these studies have resulted in the so called quasar main sequence (see [Marziani et al., 2018](#), [Sulentic & Marziani, 2015](#))

In this work, we have compiled a representative sample of NLSy1 galaxies and BLSy1 galaxies and performed a statistical study based on the various physical parameters responsible for driving the variations in both types of galaxies. The primary objective of current study is to understand the diversity observed in the physical parameters for a representative sample of both broad line and narrow line Seyfert-1 galaxies and its correlation with the physical parameters obtained through optical and X-ray observations, and then establish a comparison between the two types of galaxies based on these parameters.

2. Data and fitting procedure

A sample comprising of both BLSy1 and NLSy1 galaxies with almost similar luminosity and matching in the redshift domain has been assembled in order to study the properties of these two seemingly different classes of galaxies. More information about this sample is available in [Ojha et al. \(2020b\)](#). The single epoch optical spectrum for all the sources was obtained from the SDSS archives (see [Rakshit et al., 2017](#), [Shen et al., 2011](#), [York et al., 2000](#), etc.) using the SDSS-SAS DR16 server¹. For all the sources we performed a search query for the optical spectrum on the SDSS-SAS server for a region around 0.05 arc minutes within the specified Right Ascension (RA) and Declination (DEC) positions of these sources. The spectra were brought to the rest frame using the redshift values available in the

¹<https://dr16.sdss.org/optical/spectrum/search>

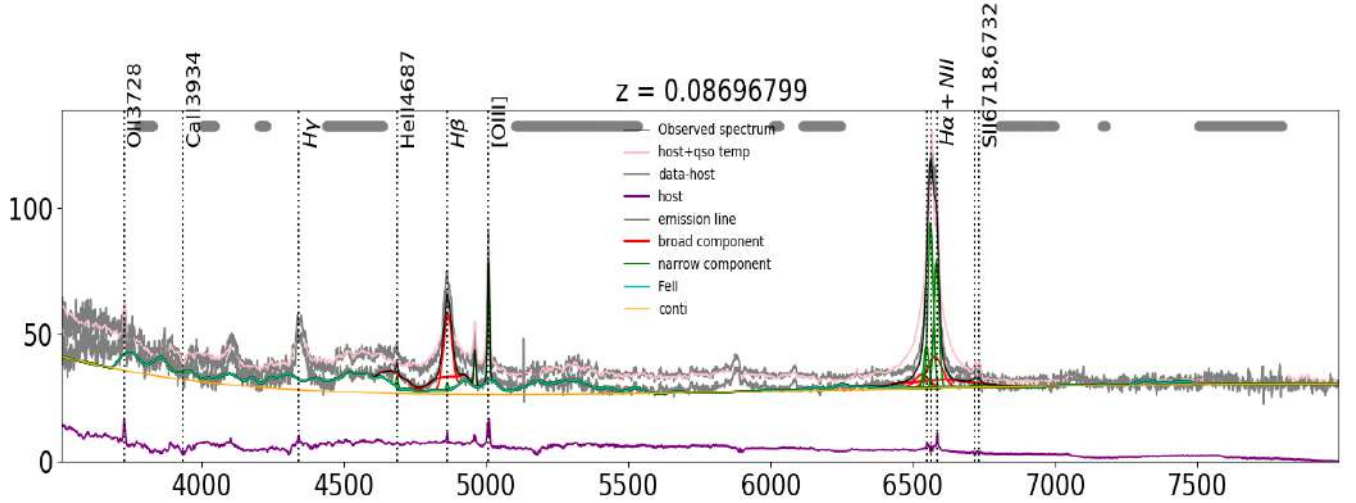


Figure 2. Demonstration of the fitting procedure. The continuum has been fit using a power law, the emission lines have been fit using a combination of gaussians, the host galaxy has been decomposed using already available template in Yip et al. (2004) and the Fe blend has been removed using the templates available in Boroson & Green (1992).

header of the individual FITS files obtained from SDSS DR16. A limit of Signal to Noise Ratio (SNR) ≥ 5 was put for identifying the emission lines clearly. Out of the 225 NISy1 galaxies in the sample, the SNR criteria reduced 10 sources while out of 164 BLSy1 galaxies from the sample, this criterion reduced 14 sources.

PyQSOFIT², a publicly available code to fit the quasar spectra has been used to analyse the individual spectra. It is written in Python language, and has been used for fitting the SDSS quasar spectra recently (see Gaur et al., 2019, Rakshit et al., 2020, etc.). Initially, the continuum model is prepared using the host galaxy components, contribution from the iron line and the accretion disk emission which reflects itself as a power law component (see Figure 2). We removed the host galaxy component using the PCA method, obtained from the host galaxy templates of (Yip et al., 2004). For many of the sources in our sample the host galaxy decomposition could not be applied. The FeII blends were removed using the templates available in Boroson & Green (1992) which are available within the code itself. The accretion disk component was fitted as a polynomial and the final continuum model was subtracted from the original spectrum, which yielded the emission line components only. We were concerned with measuring the asymmetry in the $H\beta$ emission line, hence for the emission line fitting, we concentrated on the $H\beta$ -OIII complex only. We assumed the emission line complex to be composed of a narrow and a broad central component representing the $H\beta$ emission arising from the Narrow line and Broad line regions respectively. The width of the narrow Gaussian components used for fitting the OIII doublet, was tied with the narrow component of the $H\beta$ emission line which physically indicates the emission coming from the same narrow line region. The limits for the width of the Gaussian profiles were set as 800 km/sec for narrow components, up to 2300 km/sec for broad components and beyond 10000 km/sec for very broad components for fitting the NISy1 galaxies. The limit of 2300 km/sec was kept keeping in mind the previous works classifying the NISy1 galaxies (for example, see Rakshit et al., 2017). For fitting the BLSy1 we removed the upper limit of 2300 km/sec on the broad component, while still allowing up to three Gaussian profiles including a very broad component. Out of 225 NISy1 galaxies, we could fit and get proper measurements of physical quantities for 144 sources, while out of 164 BLSy1 galaxies, we could fit and get proper measurements for 110 sources.

²<https://github.com/legolason/PyQSOFit>

3. Analysis

We obtained the physical parameters from the spectral fitting and derived a few parameters based on empirical relations. The FWHM of the $H\beta$ emission line, area covered by the line, and its equivalent width (EW) were obtained from the direct decomposition of the spectra. The area covered by the $H\beta$ emission line was calculated by integrating the flux between 4700Å and 4920Å. We calculated the equivalent width (EW) of the emission line using the same wavelength window and the monochromatic luminosity at 5100 Å (L_{5100}) was obtained from the fit. The broad line region of NLSy1 galaxies is understood to be richer in FeII content as compared to the general population (Panda et al., 2019). The iron strength (R_{Fe}) was calculated as the ratio of area covered by the broad Fe line between 4433Å and 4684Å, and the area covered by the $H\beta$ emission line.

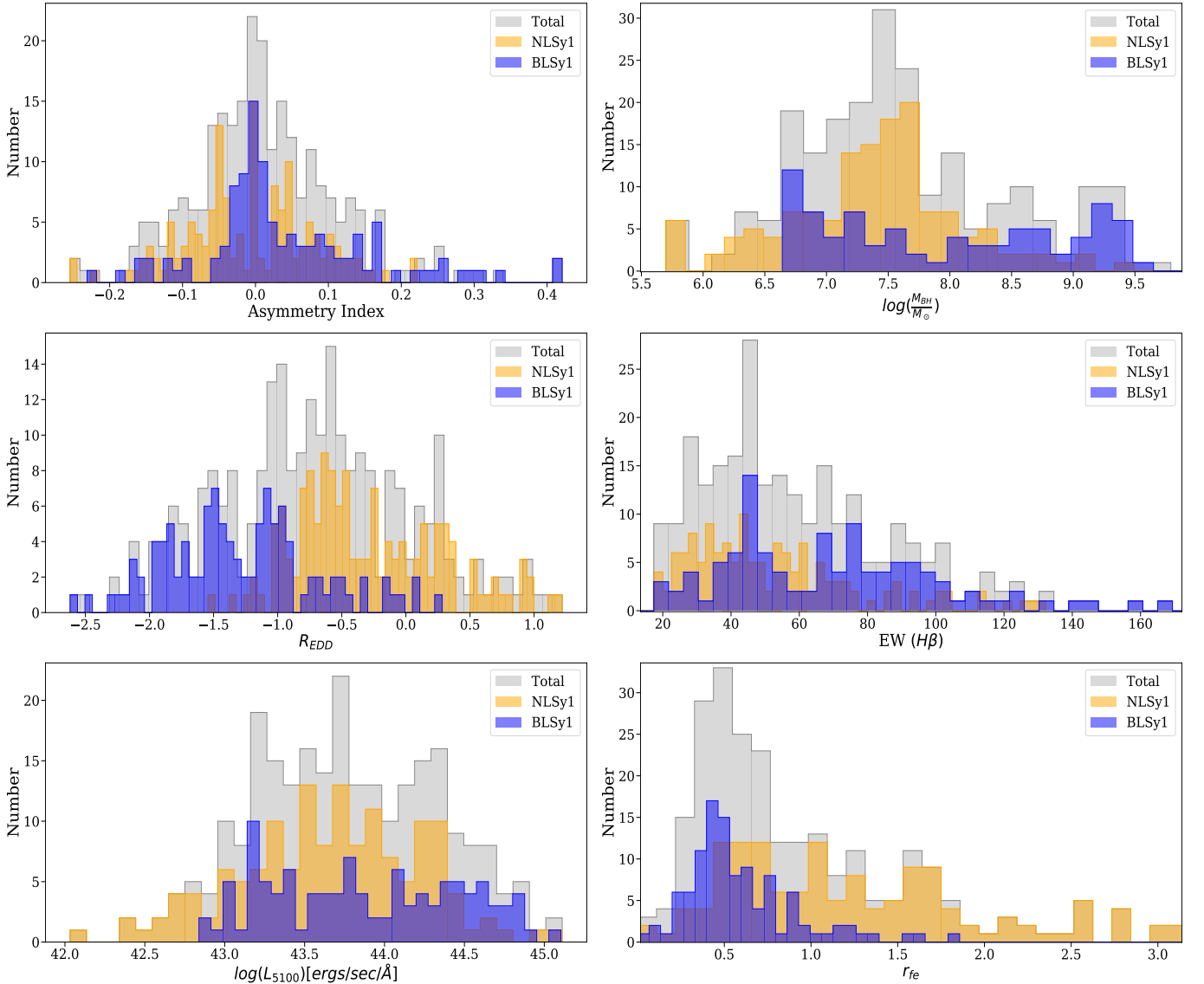


Figure 3. Distribution of various physical parameters for both the types of galaxies. Orange color denotes the NLSy1 galaxies, Blue color denotes the BLSy1 and the grey region is the combined number.

We found out the iron strength in NLSy1 galaxies to be higher than the BLSy1 galaxies for most of the AGN. The median R_{Fe} was 1.13 for the NLSy1 galaxies while it was less than half of that value, 0.49 for the BLSy1 galaxies. We estimated the flux ratio of the narrow OIII component to the broad $H\beta$ in order to understand the influence of the $H\beta$ on the emission from NLR gases. The NLSy1 galaxies have weak OIII emission and thus the OIII/ $H\beta$ ratio was lower compared to the BLSy1 galaxies. Also, the ratio of broad components of $H\alpha$ and $H\beta$ was calculated using the area covered by the broad components of the two emission lines.

The central black hole mass has been estimated using various empirical relations in the recent past. Reverberation mapping based masses provide tighter constraints on the Supermassive Black Hole (SMBH) mass and thus far this technique has been the only reliable one for SMBH mass estimation to higher redshifts (Bentz et al., 2009). The single epoch SMBH mass estimation technique is based on the scaling relations obtained from local galaxy stellar velocity dispersion.

$$M_{BH} = f_{BLR} \frac{R_{BLR}(\Delta v)^2}{G} \quad (1)$$

In this equation, R_{BLR} is the BLR radius in light days and is estimated using the so called Radius Luminosity (R-L) relation available for a set of approximately 120 reverberation mapped AGN so far (Bentz et al., 2009, Du & Wang, 2019), Δv is obtained from the FWHM of the emission line being used for the SMBH mass estimation, assuming that the gas is in virialized motion around the SMBH. The NLSy1 galaxies have smaller SMBH mass, owing to the small FWHM of the $H\beta$ emission line.

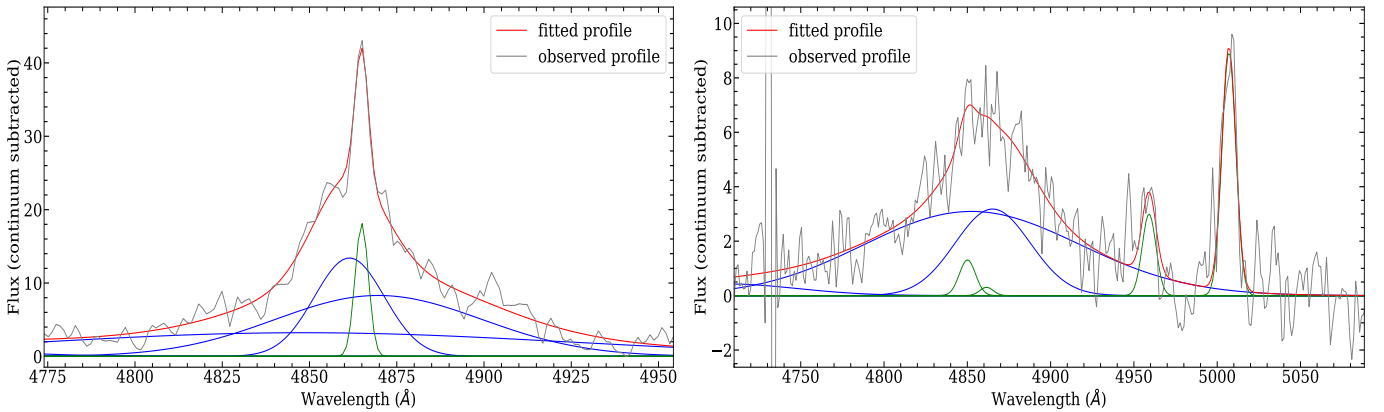


Figure 4. Example of blue (left) and red (right) asymmetric $H\beta$ profiles with AI values -0.14 and +0.12 respectively

The NLSy1 galaxies have been known to have higher accretion rates as compared to the BLSy1, which makes it one of the defining parameters in the classification. These AGN are understood to be younger in age but accreting very fast. In the eigenvector formalism of Boroson & Green (1992), the Eddington ratio, $R_{Edd} = \frac{L_{BOL}}{L_{Edd}}$ is understood to drive the variations in the parameters. The Eddington ratio is also interpreted as the age of the AGN in some recent works (Grupe, 2004). We estimated the Eddington ratio using optical spectra itself. In Ojha et al. (2020b), R_{Edd} was calculated using X-ray observations which was consistent with the estimation from that obtained from optical parameters hence we did not attempt to estimate R_{Edd} using other methods.

The asymmetry index has been used to trace the signatures of inflowing or outflowing gas in the broad line region of AGN. While the outflow asymmetry in the CIV line, known as the *blueshifting* is well known and documented (Gaskell & Goosmann, 2013) and possibly explained by the so called 2 component BLR model, the cause of similar asymmetry in a low ionisation line like $H\beta$ has not been known very well in the literature, although asymmetric $H\beta$ profiles have been known to exist. The characterisation of the AGN in terms of their emission line shapes and shifts and their correlation with physical parameters such as accretion rate etc. has been attempted in (Zamfir et al., 2010) where they conclude that the AGN with $H\beta$ FWHM ≥ 4000 km/sec show different characteristics than the ones with lower value of FWHM. We estimated the asymmetry indices for all the AGN in our sample. It has been calculated with different flux values in the recent past (Brotherton, 1996, Marziani et al., 1996). We chose a combination of 75% and 25% flux values to estimate the asymmetry index based on previous works. Basically the wavelength at which the broad emission line flux values reach the 75% and 25% of the flux values is recorded and the asymmetry index (AI) and Kurtosis Index (KI) are calculated. The correlation of AI with various physical parameters is shown in Figure 5. We also obtained the soft X-ray photon index as it is one of the fundamental components in the 4DE1 formalism. The X-ray photon indices were obtained from (Ojha et al., 2020b). The comparison between X-ray photon indices and the BLR asymmetry provides clues to the connection of the corona

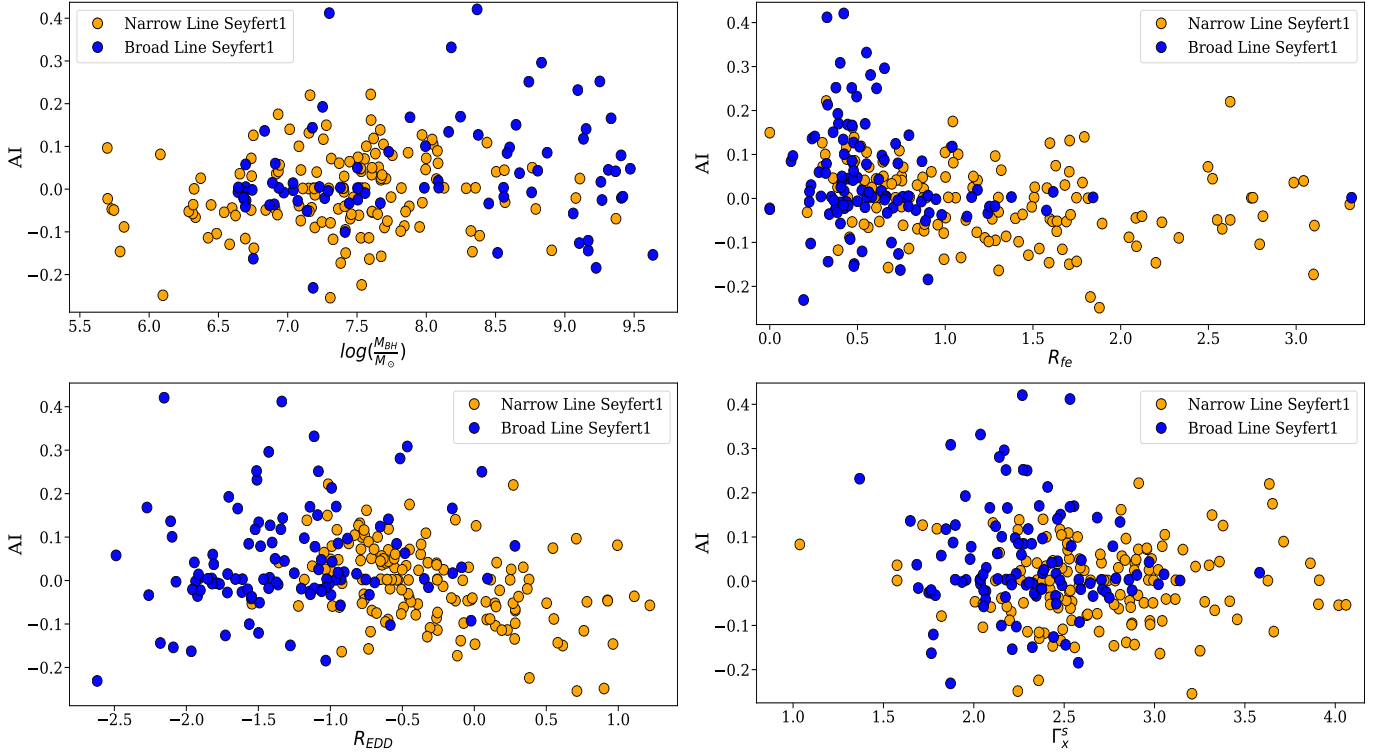


Figure 5. Correlation of asymmetry indices with various parameters for NLSy1 (orange) and BLSy1 (blue) galaxies.

in the accretion disk with the BLR. The distribution of the various parameters for the entire sample of BLSy1 and NLSy1 is presented in Figure 3. To understand the correlation among the various derived parameters, we calculated the spearman rank correlation coefficients. It is a statistical technique used to find out the strength and the direction of the association between two variables.

4. Results

The direct correlations point to higher anti correlation of the $H\beta$ FWHM with R_{fe} and R_{Edd} in the NLSy1. While there is a strong anti correlation of FWHM with R_{fe} in both the cases, it is slightly weaker in the case of BLSy1 galaxies. This may be because of the fact that R_{fe} is strongly dependent on the flux of the iron emission line and thus the emission region of NLSy1 being richer in iron content as compared to the BLSy1. The Eddington ratio is anti correlated with the $H\beta$ FWHM with the anti correlation coefficient of -0.43 for the whole sample. When the correlation is calculated separately, a positive correlation of +0.33 is present in the case of BLSy1 while it is highly anti correlated with the FWHM of $H\beta$ in the case of NLSy1 galaxies, it's correlation coefficient being -0.84. Most of the NLSy1 galaxies have higher Eddington ratios but lower FWHM than the BLSy1 hence, this skews the results for entire population in the favour of NLSy1 galaxies in this analysis.

More NLSy1 galaxies show blue asymmetries as compared to the BLSy1, which seems quite interesting. Blue asymmetries means there is outflowing gas arising from that region. In the literature (see Panda et al., 2019, Wolf et al., 2020) it has been recently known that the NLSy1 galaxies show more traces of outflow. The FWHM of $H\beta$ correlates positively, although weakly with the asymmetry index. The correlation coefficient is 0.26 in the case of BLSy1 galaxies while it comes out to be 0.37 in the case of NLSy1 galaxies. Also it is anti correlated with R_{Fe} in both the cases of NLSy1 galaxies and BLSy1 galaxies. There has been a postulation to use the AI in the emission profile as a surrogate parameter in the 4DE1 formalism. The asymmetry index shows weak correlations and anti correlations with the other known parameters. Thus, we can't conclusively determine the asymmetry index to be a dominating factor in the AGN classification based on this analysis. Soft X-ray photon index has been one of the components of the 4DE1 formalism of Boroson & Green (1992) hence we tried to correlate

it with other known parameters for this sample. Surprisingly, there is very weak correlation of the soft X-ray photon index with all the parameters in both the cases.

We tried to see if the differences in physical properties arise even when the NLSy1 galaxies are compared to the general Seyfert galaxies population. Naturally with the NLSy1 galaxies occupying extreme ends in some parameters space, it becomes imperative to understand the properties of these galaxies. In Grupe (2004), and more recently Ojha et al. (2020b) and Waddell & Gallo (2020) the properties of NLSy1 galaxies have been studied comparatively with BLSy1 galaxies. In Grupe (2004), a sample of 110 X-ray selected galaxies was available, which is around 250 in our case, owing to the availability of SDSS spectrum. The results between the two studies are largely consistent. We conclude from this work that the NLSy1 galaxies are richer in iron content (indicated by their high R_{fe} values), accrete very fast and show more traces of outflow, signified by their blue asymmetries.

Acknowledgments

The authors acknowledge the financial support provided by DST-SERB (grant no: EMR 2016/001723) for this project.

References

- Bahcall J. N. J., Kozlovsky B.-Z. B.-Z., Salpeter E. E., 1972, *ApJ*, 171, 467
- Bentz M. C., Katz S., 2015, *PASP*, 127, 67
- Bentz M. C., Peterson B. M., Netzer H., Pogge R. W., Vestergaard M., 2009, *ApJ*, 697, 160
- Blandford R. D., McKee C. F., 1982, *ApJ*, 255, 419
- Boroson T. A., Green R. F., 1992, *ApJS*, 80, 109
- Brotherton M. S., 1996, Technical report, THE PROFILES OF H β AND [O III] X5007 IN RADIO-LOUD QUASARS
- Du P., Wang J.-M., 2019, *ApJ*, 886, 42
- Gaskell C., 2000, *New Astronomy Reviews*, 44, 563
- Gaskell C. M., Goosmann R. W., 2013, *ApJ*, 769, 30
- Gaskell C. M., Goosmann R. W., 2016, *Ap&SS*, 361, 67
- Gaur H., Gu M., Ramya S., Guo H., 2019, *A&A*, 631, A46
- Grupe D., 2004, *The Astronomical Journal*, 127, 1799
- Guo H., Shen Y., Wang S., 2018, PyQSOFit: Python code to fit the spectrum of quasars, Astrophysics Source Code Library (ascl:1809.008)
- Kaspi S., Smith P. S., Netzer H., Maoz D., Jannuzi B. T., Giveon U., 2000, *ApJ*, 533, 631
- Kaspi S., Smith P. S., Netzer H., Maoz D., Jannuzi B. T., Giveon U., 2002, *ApJ*, 533, 631
- Marziani P., Sulentic J. W., Dultzin-Hacyan D., Calvani M., Moles M., 1996, *ApJS*, 104, 37
- Marziani P., et al., 2018, *Frontiers in Astronomy and Space Sciences*, 5, 6
- Mathur S., 2000, *NewAR*, 44, 469
- Netzer H., 2015, *ARA&A*, 53, 365
- Ojha V., Chand H., Krishna G., Mishra S., Chand K., 2020a, *MNRAS*, 493, 3642

- Ojha V., Chand H., Dewangan G. C., Rakshit S., 2020b, [ApJ](#), **896**, 95
- Panda S., Marziani P., Czerny B., 2019, [ApJ](#), **882**, 79
- Rakshit S., Stalin C. S., 2017, [ApJ](#), **842**, 96
- Rakshit S., Stalin C. S., Chand H., Zhang X.-G., 2017, [ApJS](#), **229**, 39
- Rakshit S., Stalin C. S., Kotilainen J., 2020, [ApJS](#), **249**, 17
- Shen Y., et al., 2011, [ApJS](#), **194**, 45
- Sulentic J. W., 1989, [ApJ](#), **343**, 54
- Sulentic J. W., Marziani P., 2015, [Frontiers in Astronomy and Space Sciences](#), **2**, 6
- Sulentic J. W., Zwitter T., Marziani P., Dultzin-Hacyan D., 2000, [ApJL](#), **536**, L5
- Sulentic J. W., et al., 2017, [A&A](#), **608**, A122
- Waddell S. G. H., Gallo L. C., 2020, [MNRAS](#), **498**, 5207
- Wang J.-M., Du P., Brotherton M. S., Hu C., Songsheng Y.-Y., Li Y.-R., Shi Y., Zhang Z.-X., 2017, [Nature Astronomy](#), **1**, 775
- Wolf J., et al., 2020, [MNRAS](#), **492**, 3580
- Yip C. W., et al., 2004, [AJ](#), **128**, 585
- York D. G., et al., 2000, [AJ](#), **120**, 1579
- Zamfir S., Sulentic J. W., Marziani P., Dultzin D., 2010, [MNRAS](#), **403**, 1759